Agmatine is transported into liver mitochondria by a specific electrophoretic mechanism

Mauro SALVI*[1], Valentina BATTAGLIA*[1], Mario MANCON*, Sebastiano COLOMBATTO†, Carlo CRAVANZOLA†, Rita CALHEIROS‡, Maria P. M. MARQUES‡, Maria A. GRILLO† and Antonio TONINELLO*[2]

*Dipartimento di Chimica Biologica, Università di Padova, Istituto di Neuroscienze del C.N.R., Unità per lo studio delle Biomembrane, 35121 Padova, Italy, †Dipartimento di Medicina e Oncologia Sperimentale, Sezione di Biochimica, Università di Torino, 10126 Torino, Italy, and ‡Unidade de Quimica-Fisica Molecular, Universidade de Coimbra, 3004-535 Coimbra, Portugal

Agmatine, a divalent diamine with two positive charges at physiological pH, is transported into the matrix of liver mitochondria by an energy-dependent mechanism the driving force of which is $\Delta\Psi$ (electrical membrane potential). Although this process showed strict electrophoretic behaviour, qualitatively similar to that of polyamines, agmatine is most probably transported by a specific uniporter. Shared transport with polyamines by means of their transporter is excluded, as divalent putrescine and cadaverine are ineffective in inhibiting agmatine uptake. Indeed, the use of the electroneutral transporter of basic amino acids can also be discarded as ornithine, arginine and lysine are completely ineffective at inducing the inhibition of agmatine uptake. The involvement of the monoamine transporter or the existence of a leak pathway are also unlikely. Flux-voltage analysis and the determination of activation enthalpy, which is dependent upon the valence of agmatine, are consistent with the hypothesis that the mitochondrial agmatine transporter is a channel or a single-binding centre-gated pore. The transport of agmatine was non-competitively inhibited by propargylamines, in particular clorgilyne, that are known to be inhibitors of MAO (monoamine oxidase). However, agmatine is normally transported in mitoplasts, thus excluding the involvement of MAO in this process. The I_2 imidazoline receptor, which binds agmatine to the mitochondrial membrane, can also be excluded as a possible transporter since its inhibitor, idazoxan, was ineffective at inducing the inhibition of agmatine uptake. Scatchard analysis of membrane binding revealed two types of binding site, S_1 and S_2, both with mono-co-ordination, and exhibiting high-capacity and low-affinity binding for agmatine compared with polyamines.

Agmatine transport in liver mitochondria may be of physiological importance as an indirect regulatory system of cytochrome c oxidase activity and as an inducer mechanism of mitochondrial-mediated apoptosis.

Key words: agmatine, binding kinetics, mitochondria, polyamine, transport.

INTRODUCTION

Agmatine [1-(4-aminobutyl)guanidine], the biogenic amine formed by the decarboxylation of arginine catalysed by ADC (arginine decarboxylase), is known to bind to α_2-adrenergic and imidazoline receptors, and to have properties as a neurotransmitter or neuromodulator (for review see [1]). Clinical properties have been suggested, such as a neuroprotective effect, the counteraction of tolerance to opiates [2] and tumour suppression [3]. Many other biochemical effects have also been shown: for instance, agmatine induces the ornithine decarboxylase antizyme [4,5] and SSAT (spermidine/spermine acetyltransferase) [6] and thus influences polyamine homoeostasis; it inhibits NOS (nitric oxide synthase), most potently the inducible form [7]. It may also be a precursor to polyamines, through its hydrolysis to putrescine by AGMase (agmatinase) [8].

In mammals agmatine is not only formed 'in situ' by ADC, but may also be taken up from exogenous sources; it is known to be present in food and to be produced by the intestinal flora [9]. It follows that transport of agmatine across the plasma membrane may contribute to regulation of its cytosol concentration and therefore its biological action. Generally, after being absorbed from the stomach by means of an energy-dependent mechanism, it is taken up by several organs, but particularly by the liver [10]. The mechanism involved has been studied in various cell types such as hepatocytes in primary culture [11], endothelial [12] and kidney cells [13], and several other mammalian cell types [14] which take up agmatine using the same transporter as polyamines. By contrast, agmatine and putrescine appear to be transported by different carriers in gliomal cells [15] and in a cell line derived from human embryonic kidney, in which OCT-2 (organic cation transporter) and EMT (extraneural monoamine transporter) are used [16].

Agmatine has recently been found to be present in neuronal mitochondria [17]. ADC and AGMase have also been located to mitochondria [18–20], as well as the I_2 imidazoline receptor, which binds agmatine and, in particular is located on MAO (monoamine oxidase) [21]. All of these observations, that reveal close relationships between this amine and mitochondria, led us to examine whether agmatine could be transported into these organelles and, if so, to characterize the mechanism and establish whether uptake is mediated by a known transporter, e.g. that for polyamines.

MATERIALS AND METHODS

RLM (rat liver mitochondria) were isolated in 0.25 M sucrose and 5 mM Hepes (pH 7.4) by conventional differential centrifugation

Abbreviations used: ADC, arginine decarboxylase; AGMase, agmatinase; DMO, 5,5′-dimethyl-oxazolidine-2,4-dione; E_a, activation enthalpy; FCCP, carbonyl cyanide *p*-trifluoromethoxyphenylhydrazone; MAO, monoamine oxidase; MPT, mitochondrial permeability transition; mtNOS, mitochondrial nitric oxide synthase; P_i, inorganic phosphate; RLM, rat liver mitochondria; TEA, tetraethylammonium; TPP^+, tetraphenylphosphonium; $\Delta\Psi$, electrical membrane potential; $\Delta\mu_H^+$, transmembrane electrochemical gradient.

[1] These authors contributed equally to this work.

[2] To whom correspondence should be addressed (email antonio.toninello@unipd.it).

[22]. Mitochondrial protein concentration was assayed by a biuret method with BSA as a standard [23].

Incubations were carried out at 20 °C with 1 mg of mitochondrial protein/ml in the following standard medium: 250 mM sucrose, 10 mM Hepes/HCl (pH 7.4), 5 mM succinate and 1.25 μM rotenone. Sodium salts were used. Other additions are indicated in the description of specific experiments. A sucrose-based medium was chosen in order to compare the results obtained with those for polyamine transport (for a review, see Toninello et al. [24]). However, the effects of higher ionic-strength media are also reported (Figure 2, inset B). Uptake of [^{14}C]agmatine and [^{14}C]spermine was determined by a centrifugal filtration method, as previously described [25]. Uptake of [^{14}C]agmatine was also measured by an HPLC method [11] (demonstrating a similar trend to that mentioned above), as well as the presence of [^{14}C]guanidobutyric aldehyde and [^{14}C]putrescine in RLM. Hydrogen peroxide formation was measured fluorimetrically by the scopoletin method [26]. $\Delta\Psi$ (electrical membrane potential) was measured in an open, thermostatically controlled, stirred vessel by monitoring the distribution of the lipophilic cation TPP^+ (tetraphenylphosphonium) across the mitochondrial membrane with a selective electrode, prepared in our laboratory according to published procedures [27,28], and an Ag/AgCl reference electrode. $\Delta\Psi$ values were corrected as proposed by Jensen et al. [29]. Mitochondrial matrix volume was calculated from the distributions of [^{14}C]sucrose and ^3H_2O according to the method of Palmieri and Klingenberg [30]. ΔpH was calculated from the distribution of DMO {[^{14}C]5,5′-dimethyl-oxazolidine-2,4-dione} across the mitochondrial membrane [31].

Kinetic parameters from initial rate measurements were estimated by applying the analysis reported by Reich et al. [32]. Binding parameters were calculated by applying thermodynamic treatment of ligand receptor interactions [33]. Scatchard analyses were performed using eqn (1):

$$\frac{[B]}{[F]} = \sum_{i=1}^{s} \{[B_{max,i}] - [B_i]\} \cdot \left[\frac{1}{K_{i,1(t)}} + \varepsilon_i(F) \right] \quad (1)$$

where:

$$\varepsilon_i(F) = \sum_{k=2}^{n_i} \frac{[F]^{k-1}}{\prod_{j=1}^{k} K_{i,j}(t)}$$

represents the appropriate measure of the extent of multiple coordination on the i-th sites. $[B_{max,i}]$ is the maximum concentration of i-th sites which may be bound by the ligand, $[B_i]$ is the concentration of i-th sites bound by the ligand, $[B_{max}]$ is the maximum receptor-bound ligand concentration, [F] is the free ligand concentration; $K_{i,j}(t)$ is the affinity constant of the ligand for the i-th site, j is the occupancy number and t is time. Fitting was performed as described earlier [33].

The distribution of total bound agmatine on its binding sites was calculated by parameter $X_i(F)$, obtained by means of Eqn (2):

$$X_i(F) = \frac{[B_{max,i}] - [B_i]}{[B_{max}] - [B]} = \frac{1}{1 + \beta_i[F]} \quad (2)$$

where β_i, is a parameter describing the influence of the parallel filling of the other k-th sites in comparison with filling of the i-th site [33]. [^{14}C]agmatine was synthetized as reported in [11].

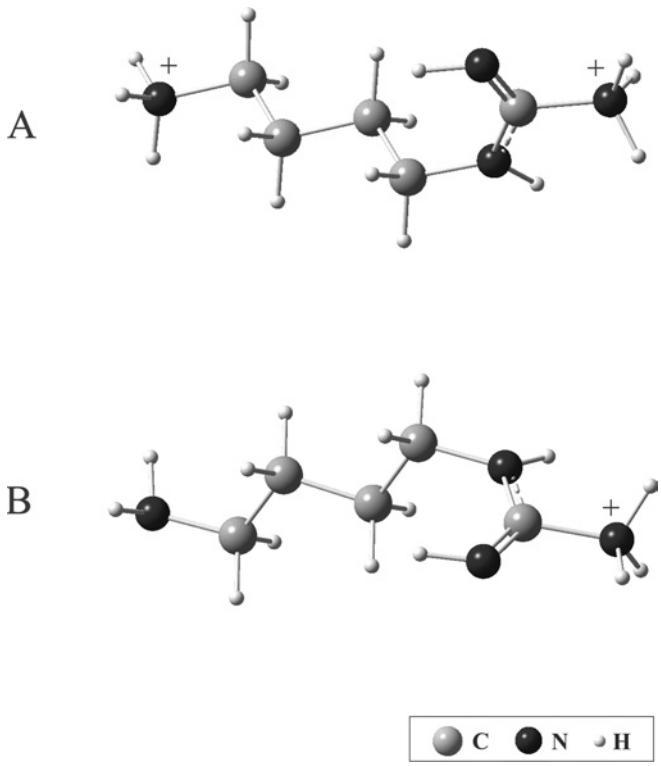

Figure 1 Agmatine structure as a divalent (A) or monovalent (B) cation

Structures were determined by *ab initio* molecular orbital calculations coupled to Raman spectroscopy [46].

RESULTS

At physiological pH, agmatine is a diamine with two net positive charges (Figure 1A), since it has the lower pKa value of 9.07 [16]. It may thus be considered as a divalent cation. Figure 1(B) shows the most stable of the monovalent forms, present at very high pH.

As shown in Figure 2, RLM incubated in standard medium take up approx. 50 nmol of [^{14}C]agmatine/mg of protein in 30 min of incubation. In the presence of FCCP (carbonyl cyanide *p*-trifluoromethoxyphenylhydrazone) or antimycin A, which completely collapses $\Delta\Psi$ (Figure 2, inset A), gradual transport of the diamine is completely inhibited. An almost identical effect is observed when the medium is deprived of succinate (results not shown). Indeed, in the presence of KCl, significant inhibition may also be observed. The inset B in Figure 2 shows the dose-dependent effect of saline-sucrose media.

It should be emphasized that no oxidation products of agmatine such as H_2O_2 or [^{14}C]guanidobutyric aldehyde were detected; nor was [^{14}C]putrescine, a catabolic product of agmatinase activity [8] (results not shown).

The inhibition of agmatine transport by de-energizing conditions indicates that it is energy-dependent and requires an $\Delta\mu_H{}^+$ (transmembrane electrochemical gradient). This observation led us to identify which component of $\Delta\mu_H{}^+$, $\Delta\Psi$ or ΔpH (or both) drives agmatine uptake i.e., to verify whether the mechanism is electrophoretic or electroneutral in nature.

Figure 3 demonstrates that in the presence of P_i (inorganic phosphate), which raises the $\Delta\Psi$ value from 150 to 180 mV (Figure 3, inset), the amount of agmatine taken up by mitochondria is approx. 80 nmol/mg of protein in 30 min of incubation. Furthermore, if RLM are incubated with the K^+/H^+ exchanger, nigericin, instead of P_i – a condition which enhances $\Delta\Psi$ up to 200 mV

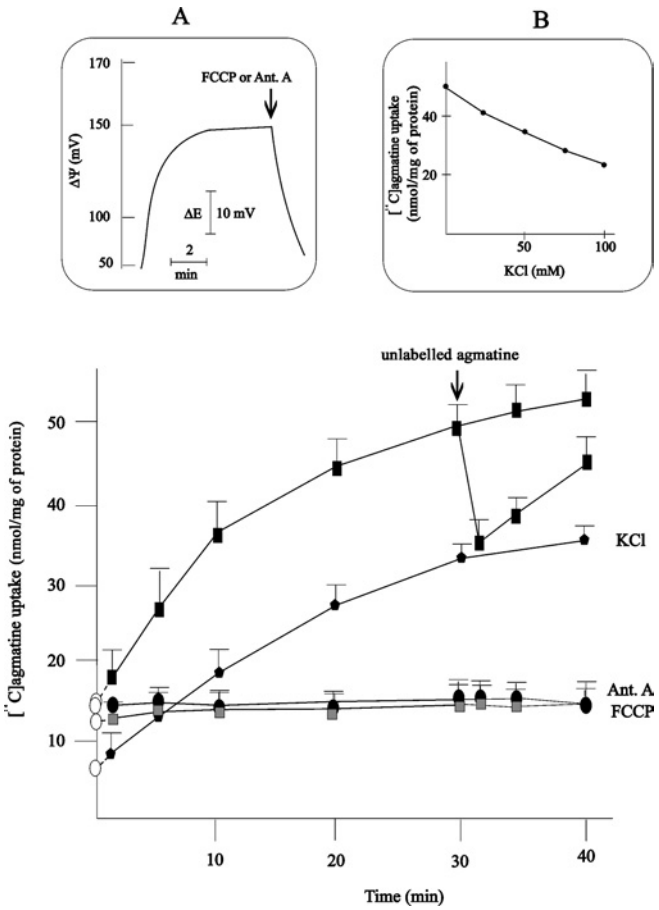

Figure 2 Agmatine uptake by rat liver mitochondria: dependence on an energized state

RLM were incubated in standard medium, as described in the Materials and methods section, with 1 mM [^{14}C]agmatine (50 μCi/mmol). When present in medium: 0.1 μg FCCP/mg of protein, or 1 μg antimycin A (Ant. A)/mg of protein, 50 mM KCl, 150 mM sucrose. Where indicated, 5 mM unlabelled agmatine was added. Dotted lines and empty circles on ordinate axis indicate the extrapolation of agmatine binding at zero-time. Values are the means $\pm$ S.D. of five experiments. Inset (**A**), de-energizing effect of FCCP and Ant. A, obtained by incubating RLM in standard medium without agmatine. ΔE, electrode potential. Inset (**B**), dose-dependent inhibition by KCl on agmatine transport. RLM were incubated in standard medium, final concentration together with sucrose was maintained at 250 mOsM. Results show amount of agmatine uptake after 30 min of incubation.

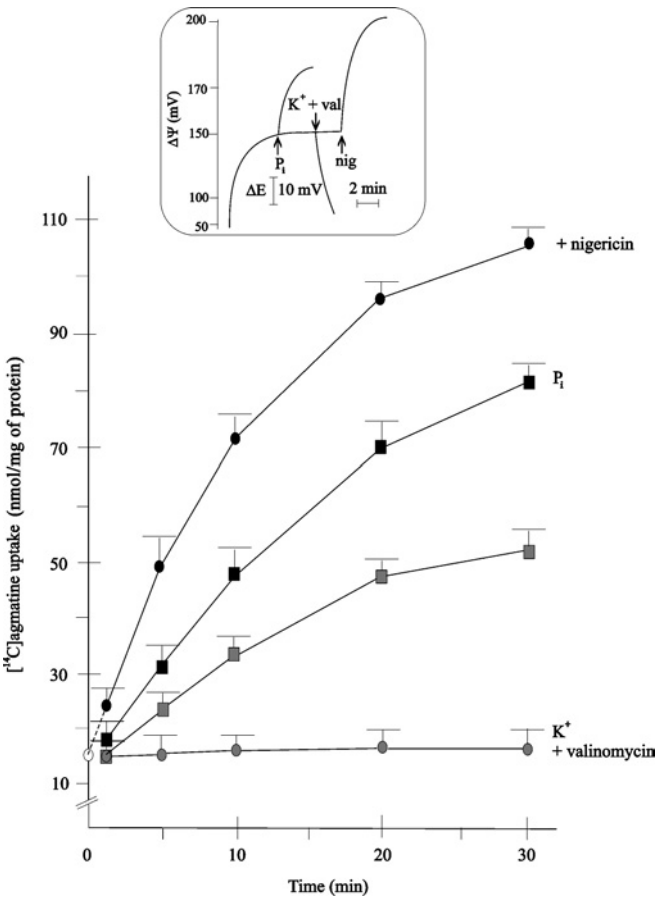

Figure 3 Effect of phosphate, nigericin, and valinomycin + K^+ on agmatine uptake and flux-voltage relationships

RLM were incubated in standard medium containing 1 mM [^{14}C]agmatine (50 μCi/mmol). When present in the medium, 1 mM P_i, 0.33 μg of nigericin (nig)/mg of protein, 0.33 μg of valinomycin (val)/mg of protein, and 10 mM KCl. Empty circles on the ordinate axis indicate agmatine bound at zero-time. Values are the means $\pm$ S.D. of six experiments. Inset, results obtained without agmatine, showing changes in $\Delta\Psi$ due to different effectors.

(Figure 3, inset) and completely collapses ΔpH – agmatine uptake is further increased in both initial rate and final extent. In contrast with the effect of P_i and nigericin, the treatment of RLM with the ionophore valinomycin, in the presence of K^+ – a condition which completely collapses $\Delta\Psi$ (Figure 3, inset) and raises ΔpH – completely inhibits the uptake of the diamine (Figure 3), as in the de-energizing conditions of Figure 2. Figure 3 clearly demonstrates that agmatine transport by RLM is electrophoretic and excludes the involvement of ΔpH. This statement is further confirmed by the gradual drop in the $\Delta\Psi$ value by approx. 20 mV after 20 min of incubation, which is paralleled by an identical increase in the 58 ΔpH value upon the addition of agmatine to RLM (Figure 4), which also demonstrates that agmatine transport occurs in conditions of high $\Delta\mu_{H^+}$ and that the driving force is $\Delta\Psi$.

The results of Figure 5(A) show the dependence of the initial rate of agmatine transport on $\Delta\Psi$, which exhibits non-ohmic conductance comparable to that of divalent putrescine [34]. A first consideration arising from this comparison is that agmatine exhibits significantly higher initial rates of transport than putrescine with increasing $\Delta\Psi$ values. The equation for influx rate J into the mitochondrial matrix of a cation is:

$$J = J_0 e^{z\beta F\Delta\Psi/RT} \quad (3)$$

where J_0 is the exchange flux (transport rate at $\Delta\Psi = 0$), z is the amine valence, and β is a parameter giving the shape and position of the energy barrier(s) for cation transport. It should be noted that, for sharp barriers, β equals the fractional distance from the external side of the membrane to the peak of the first barrier [35].

The observation of an apparently exponential relationship between agmatine transport and $\Delta\Psi$ means that flux-voltage analysis can be applied to its transport, as also previously carried out for the polyamines [34], and also in the present study re-calculated for putrescine for the best comparison. In this regard, Figure 5(B) shows the semi-logarithmic plot of the data in Figure 5(A). This gives an estimate of rate constant k and intrinsic permeability coefficient P, since $J_0 = kc$ (J_0 is the intercept of the curves on the ordinate axis, c is the concentration of the cation in the medium) and $P = k/400$ (400 is the inner membrane surface area measured in cm^2/mg of protein [36]). Assuming that agmatine can cross the membrane with its net charge at pH 7.4, 1.98 (the pK values

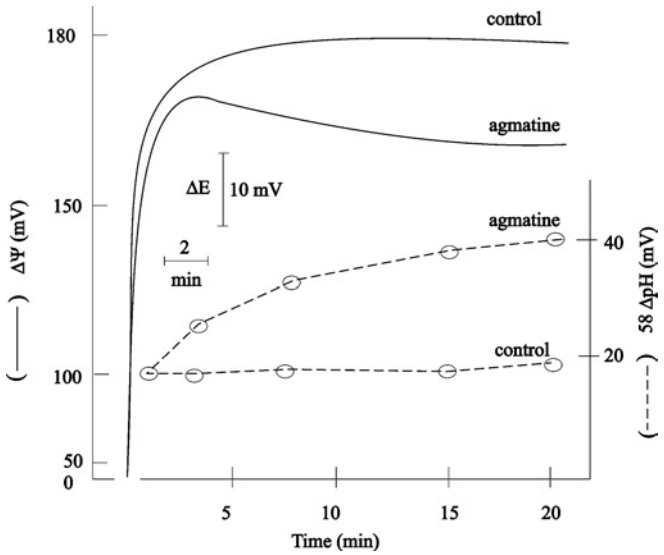

Figure 4 Changes in $\Delta\Psi$ and 58ΔpH values induced by agmatine uptake

RLM were incubated in standard medium, with 1 mM P_i, 2 μM TPP^+, 400 μM [^{14}C]DMO (1 μCi/mmol) and 5 mM [^{3}H]glycerol (100 μCi/mmol). Where indicated, 1 mM agmatine was added. Both measurements of $\Delta\Psi$ and ΔpH were performed on the same sample. A representative experiment is shown. Six other experiments gave almost identical results.

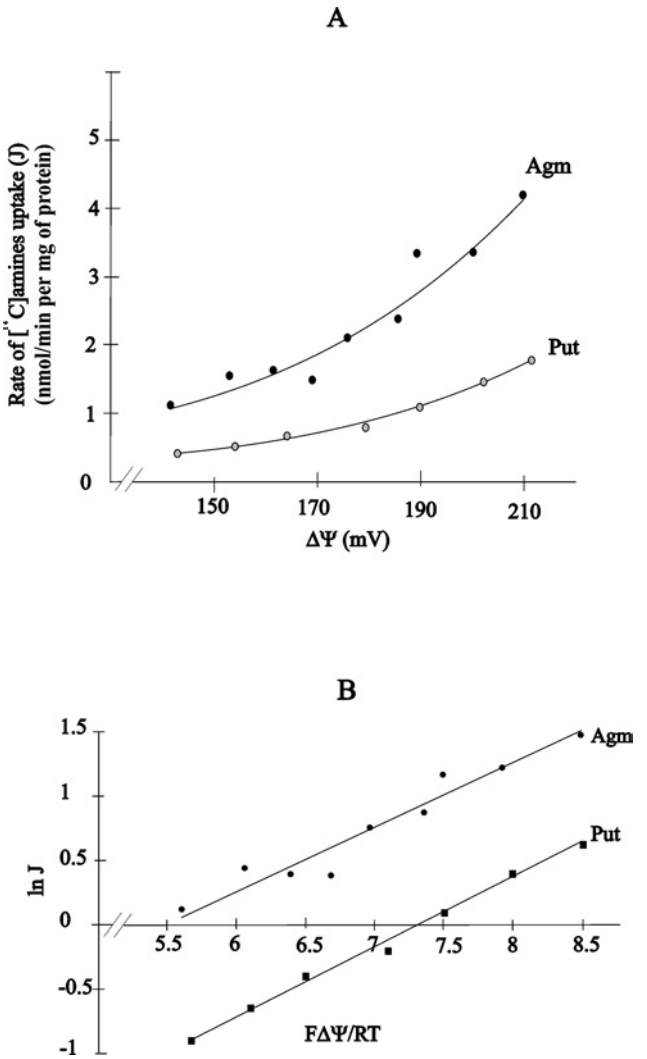

Figure 5 Flux-voltage relationship and flux-voltage analyses for agmatine and putrescine

(**A**) Agmatine and putrescine fluxes (nmol/min per mg of protein) (J) plotted, versus $\Delta\Psi$. RLM were incubated for 5 min in standard medium with 1 mM P_i, [^{14}C]agmatine, or [^{14}C]putrescine (50 μCi/mmol) at 1 mM concentration. $\Delta\Psi$ was manipulated by including limiting amounts (5–60 nM) of FCCP. The highest values of amine uptake were achieved by adding nigericin (0.33 μg/mg of protein.). Amine uptake values are corrected for instantaneous electrostatic binding [28]. The uptake of agmatine and putrescine was linear over the incubation period. A representative experiment is shown. Six experiments were carried out with each compound, yielding almost identical results. Agm, agmatine, Put, putrescine. (**B**) Log-linear plots of the data in (A). Linear regression analysis yielded values for the slopes of the curves representing product $z\beta$ (see Eqn 3). The intercepts of curves on the ordinate axis gave values of ln J_0. Agm, agmatine, Put, putrescine.

of agmatine are 9.07 and >13 [16]), and also as a monovalent cation, the value of β can be estimated from the relative slope $z\beta$ of the curves shown in Figure 5(B). All of the above parameters for agmatine and putrescine are listed in Table 1.

The β value of agmatine, 0.25, is very close to those of putrescine and the other polyamines [34] and is the theoretical value for a channel [35]. Instead, the value of β 0.5, is more appropriate for leaks or carriers (see below). The initial rate of agmatine transport was also measured at varying temperatures from a linear Arrhenius plot in the range 5–35 °C (Figure 6). The resulting slope gives the E_a (activation enthalpy) for agmatine transport. The value obtained of 22.5 kJ/mol is very close to that previously calculated for putrescine (24 kJ/mol) [34]. Also of note is the fact that the E_a/mol per charge of agmatine (E_a/z), which is 11.25 kJ, is very close not only to that of putrescine (12 kJ) but also to those of spermidine (10.6 kJ) and spermine (14.5 kJ) [34].

In mitochondrial preparations with $\Delta\Psi$ values of approx. 180 mV (in the presence of P_i), agmatine transport exhibits saturation kinetics, as illustrated by the apparent hyperbolic curve obtained in a typical experiment (Figure 7A). Estimation of kinetic parameters from initial rate measurements gives K_m and V_{max} values of 0.7 mM and 6.32 nmol/min per mg of protein respectively. For comparison, the K_m and V_{max} of putrescine transport are 1 mM and 1.14 nmol/min per mg of protein respectively [34]. All of these observations indicate that the transporter for agmatine may be the same as that for polyamines [28,34].

The experimental results shown in Figure 8 aim to solve this question and to verify whether agmatine also uses other transporters e.g., those of basic amino acids, monoamines or other monovalent cations. In this regard, polyamines and the above-mentioned cationic molecules, were used as possible inhibitors of agmatine transport. Figure 8(A) demonstrates that putrescine and cadaverine, which are also divalent at 1 mM, the same concentration used for agmatine, completely fail to inhibit the transport of agmatine. It should be noted that both polyamines inhibit the initial binding of agmatine. Figure 8(A) also shows that tetravalent spermine, at the same 1 mM concentration, exhibits marked

Table 1 Flux-voltage analyses of agmatine transport

z is the net charge of the transported amines at pH 7.4; β is the fractional distance from the external side of the membrane to the energy barrier peak, as described in eqn 1; J_0 is the exchange flux; P is the intrinsic permeability coefficent [35]. The values reported for β and J_0 are the means $\pm$ S.D. of eight experiments.

	Parameter			
Amine	z	β	J_0 nmol/mg per min	P cm/s
Agmatine	+1.98	0.25 $\pm$ 0.05	64.31×10^{-3}	26.8×10^{-10}
Agmatine	+1.00	0.5 $\pm$ 0.1	64.31×10^{-3}	26.8×10^{-10}
Putrescine	+1.99	0.27 $\pm$ 0.04	19.04×10^{-3}	7.93×10^{-10}

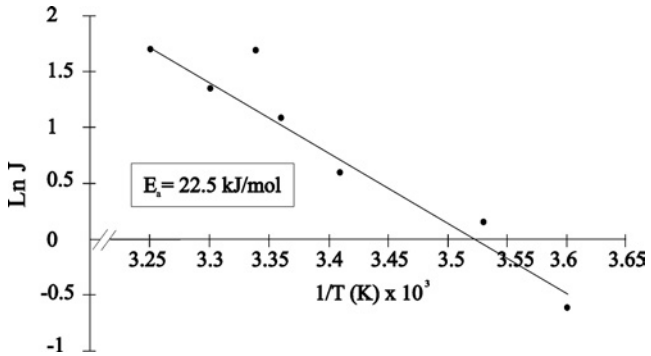

Figure 6 Arrhenius plot of agmatine transport

RLM with $\Delta\Psi$ 180 mV were incubated for 5 min over temperature range of 5–35 °C in standard medium with 1 mM P_i, [^{14}C]agmatine (50 μCi/mmol) added at 1 mM. Binding correction, as in Figure 5(A). Uptake was linear over the incubation period. A representative experiment is shown. Five other experiments gave almost identical E_a values.

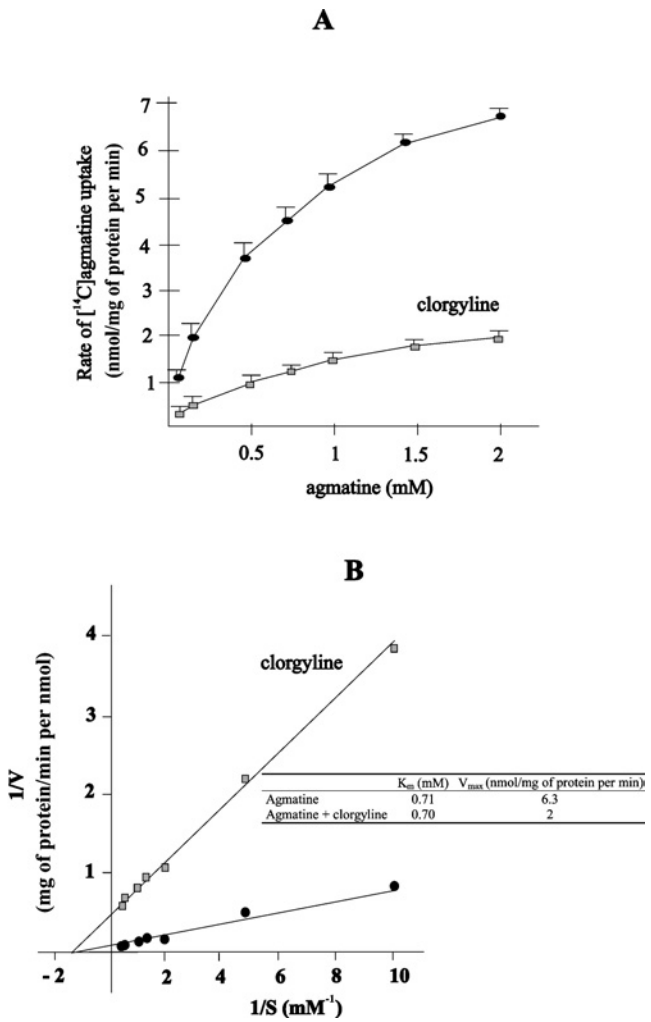

Figure 7 Saturation kinetics and double reciprocal plot of agmatine uptake. Inhibitory effect by clorgyline

(**A**) RLM were incubated for 5 min in standard medium with 1 mM P_i, and [^{14}C]agmatine (50 μCi/mmol) at the indicated concentrations. When present, clorgyline was at 1 mM. The uptake of agmatine was linear over the incubation period. Binding correction, as in Figure 5. Values are the means $\pm$ S.D. of five experiments reported. (**B**) Double reciprocal plot of the data shown in (A). Inset, the apparent K_m and V_{max} values calculated by computer simulation.

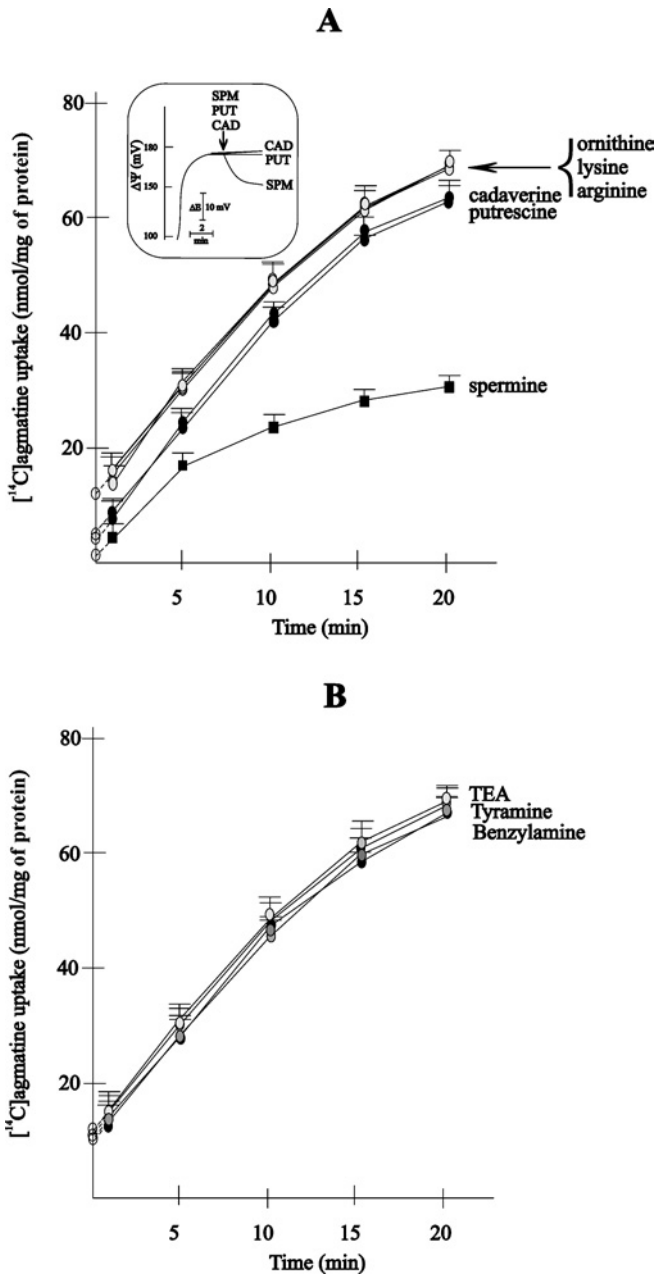

Figure 8 Effect of polyamines and basic amino acids (A), and monoamines and TEA (B) on agmatine uptake

RLM were incubated in standard medium with 1 mM [^{14}C]agmatine (50 μCi/mmol) and 1 mM P_i. When present, putrescine (PUT), cadaverine (CAD), spermine (SPM), ornithine, lysine, arginine, tyramine, benzylamine and TEA were at 1 mM concentration. Inset (**A**), the effect of polyamine transport (at 1 mM) on $\Delta\Psi$. Empty circles on the ordinate axis indicate agmatine bound at zero-time.

inhibition of this binding and transport. However, this later effect is most probably due to the fall in $\Delta\Psi$ caused by spermine transport (Figure 8A, inset), rather than to direct interaction between the two amines. It should be noted that neither putrescine nor cadaverine affect the $\Delta\Psi$ value (Figure 8A, inset). Figure 8(A) shows that agmatine transport is also not affected by 1 mM ornithine, lysine or arginine. An identical lack of efficacy is exhibited by the monoamines, tyramine and benzylamine, and the monovalent cation TEA (tetraethylammonium) (Figure 8B). None of these molecules affect $\Delta\Psi$ (results not shown).

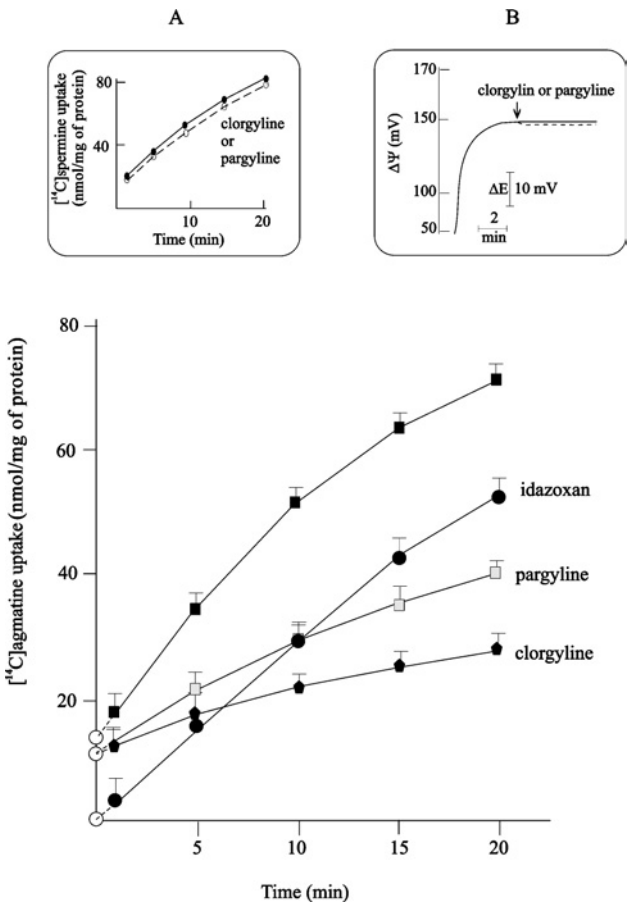

Figure 9 Effect of propargylamines and idazoxan on agmatine uptake

RLM were incubated in standard medium in the presence of 1 mM [^{14}C]agmatine (50 μCi/mmol) and 1 mM P_i. When present, clorgyline and pargyline were at concentrations of 50 and 100 μM respectively, and idazoxan at 200 μM. Empty circles on the ordinate axis indicate agmatine bound at zero-time. Insets (**A**) and (**B**), effect of propargylamines (dashed lines), at the concentrations described above, on spermine transport and $\Delta\Psi$; [^{14}C]spermine (50 μCi/mmol) at 1 mM concentration.

Figure 9 demonstrates that strong inhibition is observed with the propargylamines, pargyline and clorgyline, that are inhibitors of MAO activity. It should be emphasized that they are completely ineffective at inhibiting spermine transport (Figure 9, inset A). These inhibitors do not in fact affect $\Delta\Psi$ (Figure 9, inset B). It is noteworthy that propargylamines have a single protonated amino group [37], so that their inhibition sustains the hypothesis that agmatine is transported as a monovalent rather than a divalent cation.

As agmatine is able to bind to the I_2 imidazoline receptor located on the mitochondrial membrane [21], the experiment shown in Figure 9 was also performed with the aim of verifying whether this receptor is involved in agmatine transport. The results show that the I_2 inhibitor idazoxan does not prevent its net transport but completely inhibits the initial binding of agmatine (see the extrapolation of transport traces at zero time, Figure 9).

The observation that propargylamines strongly inhibit the transport of agmatine led us to identify the type of inhibition induced. The results of Figure 7(A) show that clorgyline, at 50 μM, causes marked inhibition of the initial rate of agmatine transport and that this inhibition is of a non-competitive type, as demonstrated by the double reciprocal plot in Figure 7(B). In this case the K_m is 0.71 mM and the V_{max} is 2.01 nmol/min per mg of protein.

All experiments reporting agmatine transport (e.g. see Figures 2, 3, 8 and 9) show that the gradual phase of agmatine accumulation (in the absence of effectors) is preceded by a phase of very rapid uptake of approx. 15 nmol/mg of protein, as calculated by rough extrapolation of the curves at zero-time (see the description of results in Figure 9). Indeed, as Figure 2 demonstrates, this uptake is sensitive to the presence of KCl. This almost instantaneous uptake is very probably due to the electrostatic binding of agmatine to the accessible surface of mitochondrial membranes, according to the following considerations: (i) it also occurs in de-energizing conditions (see Figure 2), (ii) the addition of 5 mM unlabelled agmatine during the accumulation of the labelled diamine induces the very rapid loss of an amount almost identical to that already bound at zero-time (Figure 2).

The observation that propargylamines inhibit agmatine transport with no significant inhibition of initial binding (see extrapolations at zero-time, Figure 9) and that idazoxan behaves in the opposite way, indicates that there is more than one binding site for agmatine on the mitochondrial membrane. The experiments shown in Figure 10 were performed in order to clarify this point. Figure 10(A) indicates the different amounts of agmatine that bind to the mitochondrial membrane at zero-time, as a function of the total, external agmatine concentration. As shown, binding of the amine tends towards saturation. Figure 10(B), shows the results of Scatchard analysis of agmatine binding, and demonstrates that the theoretical curve for agmatine that satisfactorily fits the experimental data (Figure 10B) is typical for two binding sites, S_1 and S_2, both with mono-co-ordination. The calculated total concentration of bound agmatine (B), 83.20 ± 0.04 nmol/mg of protein, is distributed between S_1 ($B_{max1} = 3.20 \pm 0.03$ nmol/mg of protein) and S_2 ($B_{max2} = 80.05 \pm 0.02$ nmol/mg of protein) at 3.85 and 96.15 % respectively. Dissociation constants ($K_1 = 25 \pm 3$ nmol/mg of protein and $K_2 = 4937 \pm 8$ nmol/mg of protein) of S_1 and S_2, respectively, demonstrate that S_1 has an affinity approx. 200 times higher than that of S_2. Comparisons with the binding parameters of polyamines [38] show that both sites have high binding-capacity and low-affinity.

As the targets of propargylamines and idazoxan, i.e. MAO and the I_2 receptor respectively, are located on the outer membrane, in order to establish if their effects are related to these interactions, the rate of agmatine transport was also determined in mitoplasts and compared with that in mitochondria. However, results (not shown) indicated that agmatine is taken up by mitoplasts at the same rate and to the same extent as in mitochondria, indicating that the effects of the inhibitors are not due to their interactions with the outer membrane and that the transport process involves neither MAO or the I_2 receptor.

DISCUSSION

The results described in the present study, provide evidence that agmatine is capable of binding to mitochondrial membranes and of being taken up into the matrix space of RLM. This binding, most probably electrostatic in nature, takes place in two sites, S_1 and S_2 (Figure 10), and is affected by natural polyamines (Figure 8A), idazoxan (Figure 9) and saline medium (Figure 2), and is unaffected by de-energizing agents (Figure 2), cationic amino acids (Figure 8A), monoamines or monovalent cations (Figure 8B). Agmatine binding is followed by slow, long-lasting uptake which is highly dependent on mitochondrial energization (Figures 2 and 3) and is electrophoretic in nature (Figures 3 and 4). It also exhibits a non-linear current voltage relationship (Figure 5A), in keeping with the general behaviour of monovalent and polyvalent cations (e.g. polyamines) in mitochondria [34,35].

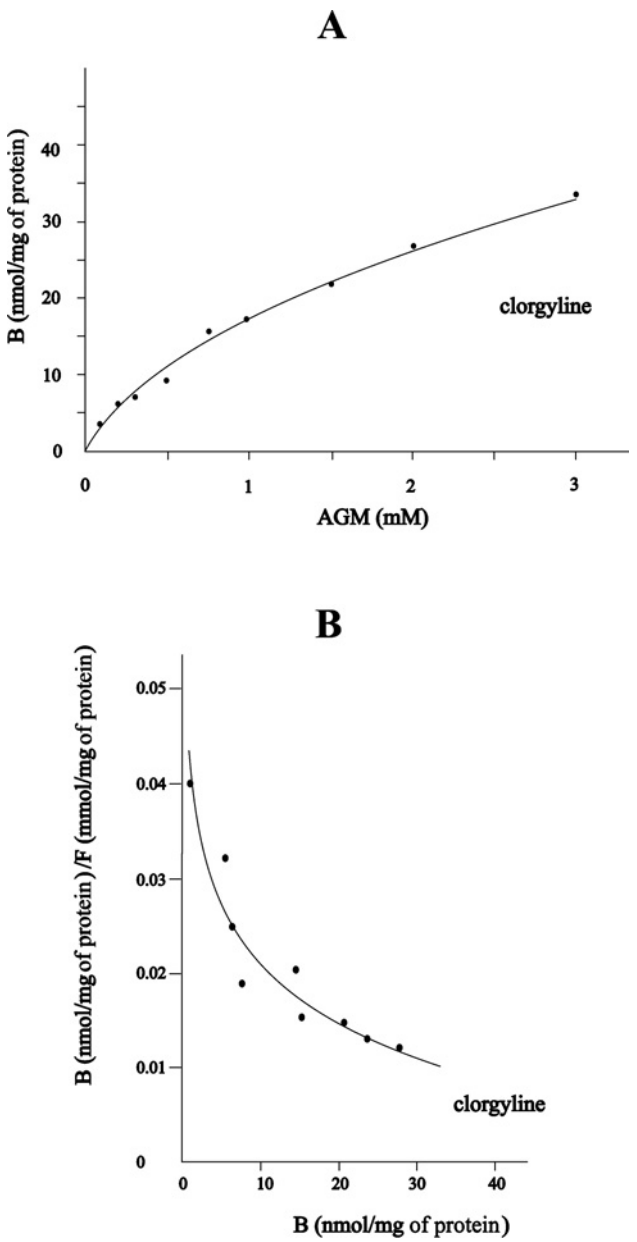

Figure 10 Binding of agmatine to energized mitochondria

(**A**) Concentration-dependent zero-time binding. Mitochondria were incubated for 3 min in standard medium, as described in the Materials and methods section, with various [$^{14}\chi$] agmatine (AGM) concentrations, in the range 100–3000 μM (0.05 μCi/ml), as indicated, and 1 mM P_i. B values were obtained by measuring agmatine uptake (nmol/mg of protein) at various times and extrapolating to zero time (on the y-axis) the trend of the curves, which is linear at all concentrations, in the first 5 min of incubation (for a more complete description, see Figure 1 in [32]). Results are representative of a typical experiment. Standard deviations of binding constants are reported in Table 1. (**B**) Binding analysis with thermodynamic treatment of Scatchard. B values (agmatine bound at zero-time) were calculated as described above; free agmatine concentration (F) was determined by subtracting bound agmatine (B) from total agmatine, shown in (A). The continuous line is a theoretical curve calculated using eqn 1 for Scatchard-based analysis, as described in the Materials and methods section.

Considering flux-voltage analysis (Figure 5), it should be noted that agmatine, depending on the valence of transported species, can exhibit two different β values (Table 1). The calculation of $\beta = 0.25$ for the divalent form, very close to those of putrescine (Figure 5B, Table 1) and the other polyamines, suggests that agmatine is transported by a channel with two energy barriers, similar to that of polyamines [34].

This possibility is also supported by the calculation of the intrinsic permeability coefficient, *P* (Figure 5, Table 1). This value, $26.8 \cdot 10^{-10}$ cm/s, is higher than that of putrescine (Table 1), and those of spermidine and spermine [34], but of the same order of magnitude. These permeabilities are very similar to that of the monovalent cation TEA – $3.54 \cdot 10^{-10}$ cm/s – which is transported by a leak pathway [34]. However, taking into account the divalency of agmatine, its permeability is very high, suggesting the presence of a uniport transporter which may be a channel.

This hypothesis is also strengthened by the E_a/z value of this uptake, which is 11.25 kJ/mol (Figure 6), i.e. very similar to that of polyamines, which have an average E_a/z value of 12.6 kJ/mol [34]. These values are much lower than that of TEA, which is 76 kJ/mol [34], and are comparable with that of the Ca^{2+} channel, which is 20 kJ/mol [39]. Indeed, the E_a for agmatine, 22.5 kJ/mol, is much lower than those of several mitochondrial carriers, which range from 64 to 92 kJ/mol [40,41].

Force-flux analysis also demonstrates that monovalent agmatine is taken up by a transport system having a β value of 0.5 [Figure 5B, Table 1]. Bearing in mind that E_a values as low as 20–30 kJ/mol have also been identified for secondary transporters in mitochondria [42–44], this β value may be applied to a single-binding centre-gated pore, of which a typical example is the ATP/ADP carrier [45]. The observation that the initial rate of agmatine transport is higher than that of putrescine (Figure 5A) but also that of the other polyamines [34] is ascribed to the fact that agmatine in its divalent form (Figure 1A) has a dipole moment, $\mu = 5.1$ D [46], whereas in polyamines $\mu = 0$. In this regard, it should be noted that the monovalent agmatine (Figure 1B) has a very high dipole moment ($\mu = 15.8$ D) [46], suggesting that this may be the predominant form involved in transport. As the pH value of the channel or gated pore environment is not known, the question of whether the monovalent or divalent form of agmatine is actually transported is not resolved. Because this information is critical for determining parameter β, the nature of the transport system still remains opent to debate.

As previously demonstrated, the polyamine transporter is common to all natural polyamines, so that they reciprocally inhibit their transport in a competitive manner [34]. Hence, putrescine, cadaverine and spermine should exhibit the same type of agmatine transport inhibition. Observations that the divalent putrescine and cadaverine are ineffective (Figure 8A), indicate the existence of different transport systems for agmatine and polyamines, rather than a single common one. Indeed, the results shown in Figure 8(A) clearly exclude the possibility that agmatine can use the electroneutral transporter of basic amino acids [47,48]. Figure 8(B) demonstrates that TEA, tyramine and benzylamine, like other monoamines (results not shown), fail to exhibit any inhibition, suggesting that the leak pathway for monovalent cations [34] and the transporter for monoamines (A. Toninello, unpublished work), both of which are electrophoretic, are not involved. Strong inhibition of agmatine transport is observed with clorgyline and pargyline, which act as non-competitive inhibitors of transport and function independently of action on MAO (Figure 9). Observations that some compounds, e.g. putrescine, cadaverine (Figure 8A) and idazoxan (Figure 9), decrease initial binding without affecting transport, whereas others, such as propargylamines, inhibit transport without inhibition of initial binding, indicate that there are at least two types of binding sites for agmatine on mitochondrial membranes. The results shown in Figure 10 clearly confirm the existence of two binding sites, S_1 and S_2, which as also observed for polyamine binding [33,38], exhibit mono-co-ordination, with high binding-capacity and low-binding affinity.

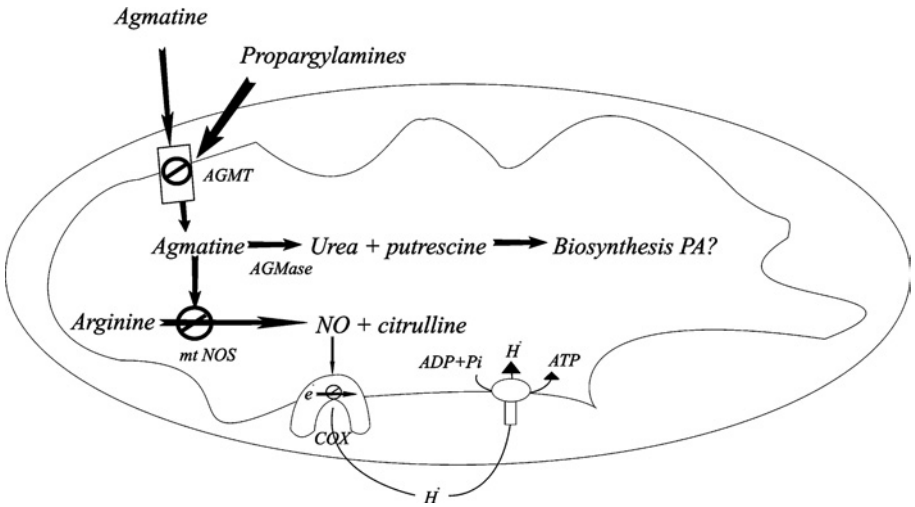

Figure 11 Proposed physiological role of agmatine in RLM

As described in the text. AGMT, agmatine transporter; COX, cytochrome c oxidase; PA, polyamines.

The non-competitive inhibition of agmatine transport exhibited by clorgyline (Figure 7B) excludes the possibility that both molecules are taken up by the same transporter. The observation that clorgyline does not completely inhibit agmatine transport (Figure 7A) is consistent with residual binding of agmatine to its transporter, putatively identified as binding site S_1. This site, in fact has the same characteristics as the polyamine binding site that is involved in transport [33].

In conclusion, we report the existence of a specific selective transport system for agmatine in RLM, which may be a channel or, alternatively, a single-binding centre-gated pore. These results are considered of physiological importance, since the agmatine concentrations used (0.1–1 mM) and the K_m calculated for transport (0.7 mM) are compatible with the concentration of agmatine normally measured in liver cells, i.e. 0.5 mM [49]. It should also be taken into account that fluctuations in this concentration may be observed in various physiological and pathological situations [7]. For example, it may increase by approx. 20×, as observed in rat aorta after ischaemic injury [50]. In particular, agmatine transport in RLM is able to induce apoptosis in hepatocytes by activating caspase 3 [51], owing to the release of cytochrome c from mitochondria promoted by agmatine, as a result of the MPT (mitochondrial permeability transition) induced in the presence of phosphate and a high Ca^{2+} concentration. It is generally believed that MPT is closely connected with programmed cell death (for recent reviews see [24,52]) the main role of which is probably to counteract tumour growth.

Another important point to be considered in evaluating the role of agmatine transport in RLM is the presence in these organelles of both biosynthetic and catabolic agmatine enzymes, such as ADC [18,19] (the presence of ADC is strongly debated [53]), and AGMase [20]. In this regard, it is noteworthy that the occurence of agmatine in cells is particularly high in liver [49]. Thus the identification of AGMase in the matrix of RLM indicates the importance of elucidating a transport system for agmatine located on mitochondria. AGMase may represent a mechanism for regulating agmatine signalling properties in RLM via changes in agmatine levels in these organelles [54].

The observation that agmatine is an inhibitor of NO synthesis [7] raises the question of the important function of agmatine and AGMase at a mitochondrial level. NO is produced by a group of NOSs (NO synthases) including three isoforms [55,56]. The mtNOS (mitochondrial NOS) isoform is constitutively present in the mitochondrial matrix, and is involved in altered mitochondrial regulation during hypoxia [57]. Indeed, mitochondrial NO has been identified as a physiological regulator of electron flux and ATP synthesis by inhibiting COX (cytochrome c oxidase) [58]. An increase in mitochondrial NO may follow the induction and activation of mtNOS, and is important in mediating mitochondrial pathology, including the effects of aging, inflammation and cancer [58]. In this regard, it should be emphasized that mtNOS activity may be regulated by changes in matrix concentration of agmatine, as the result of concerted activity by the agmatine transporter and AGMase [58]. In conclusion, the presence of agmatine in the mitochondrial matrix, if it inhibits mtNOS, favours ATP synthesis, whereas its fall in concentration as a result of AGMase activity facilitates NO production, with consequent inhibition of ATP synthesis (see Figure 11).

The present study was made possible by the award of a COST (European Science Foundation) STSM to V.B., and a PhD fellowship from the Portuguese Foundation for Science and Technology to R.C.

REFERENCES

1 Reis, D. J. and Regunathan, S. (2000) Is agmatine a novel neurotransmitter in brain? Trends Pharmacol. Sci. **21**, 187–193
2 Kolesnikov, Y., Jain, S. and Pasternak, G. W. (1996) Modulation of opioid analgesia by agmatine. Eur. J. Pharmacol. **296**, 17–22
3 Satriano, G., Kelly, C. J. and Blantz, R. C. (1999) An emerging role for agmatine. Kidney Int. **56**, 1252–1253
4 Satriano, J., Matsufuji, S., Muratami, Y., Lortie, M. J., Schwartz, D., Kelly, C. J., Hayashi, S. and Blantz, R. C. (1998) Agmatine suppresses proliferation by frameshift induction of antizyme and attenuation of cellular polyamine levels. J. Biol. Chem. **273**, 15313–15316
5 Babal, P., Ruchko, M., Campbell, C. C., Gilmour, S. P., Mitchell, J. L. and Gillespie, M. N. (2001) Regulation of ornithine decarboxylase activity and polyamine transport by agmatine in rat pulmonary artery endothelial cells. J. Pharmacol. Exper. Ther. **296**, 372–377
6 Vargiu, C., Cabella, C., Belliardo, S., Cravanzola, C., Grillo, M. A. and Colombatto, S. (1999) Agmatine modulates polyamine content in hepatocytes by inducing spermidine/spermine acetyltransferase. Eur. J. Biochem. **259**, 933–938
7 Galea, E., Regunathan, S., Eliopoulos, V., Feinstein, D. L. and Reis, D. J. (1996) Inhibition of mammalian nitric oxide synthases by agmatine, an endogenous polyamine formed by decarboxylation of arginine. Biochem J. **316**, 247–249

8 Mistry, S. K., Burnwell, T. J., Chambers, R. M., Rudolph-Owen, L., Spaltman, F., Cook, W. J. and Morris, S. M. (2002) Cloning of human agmatinase. An alternate path for polyamine synthesis induced in liver by hepatitis B virus. Am. J. Physiol. Gastrointest. Liver Physiol. **282**, G375–G381

9 Raasch, W., Regunathan, S., Li, G. and Reis, D. J. (1995) Agmatine, the bacterial amine, is widely distributed in mammalian tissues. Life Sciences **56**, 2319–2330

10 Molderings, G. J., Heinen, A., Menzel, S. and Gothert, M (2002) Exposure of rat isolated stomach and rats in vivo to [^{14}C]agmatine: accumulation in the stomach wall and distribution in various tissues. Fund. Clin. Pharmacol. **16**, 219–225

11 Cabella, C., Gardini, G., Corpillo, D., Testore, G., Bedino, S., Solinas, S. P., Cravanzola, C., Vargiu, C., Grillo, M. A. and Colombatto, S. (2001) Transport and metabolism of agmatine in rat hepatocyte cultures. Eur. J. Biochem. **268**, 940–947

12 Babal, P., Ruchko, M., Olson, J. W. and Gillespie, M. N. (2000) Interactions between agmatine and polyamine uptake pathways in rat pulmonary artery endothelial cells. Gen. Pharmacol. **34**, 255–261

13 Del Valle, A. E., Paz, J. C., Sanchez-Jimenez, F. and Medina, M. I. (2000) Agmatine uptake by cultured hamster kidney cells. Biochem. Biophys. Res. Commun. **280**, 307–311

14 Satriano, J., Isome, M., Casero, R. A., Thomson, S. C. and Blantz, R. C. (2001) Polyamine transport system mediates agmatine transport in mammalian cells. Am. J. Physiol. Cell Physiol. **281**, C329–C334

15 Molderings, G. J., Bonisch, H., Gothert, M. and Bruss, M. (2001) Agmatine and putrescine uptake in the human glioma cell line SK-MG-1. Naunyn-Schmiedeberg's Arch. Pharmacol. **363**, 671–679

16 Grundemann, D., Hahne, C., Berkels, R. and Schomig, E. (2003) Agmatine is efficiently transported by non-neuronal monoamine transporters extraneuronal monoamine transporter (EMT) and organic cation transporter 2 (OCT2). J. Pharmacol. Exp. Ther. **304**, 810–817

17 Gorbatyuk, O. S., Mihner, T. A., Wang, G., Regunathan, S. and Reis, D. J. (2001) Localization of agmatine in vasopressin and oxytocin neurons of the rat hypothalamic paraventricular and supraoptic nuclei. Exp. Neurol. **171**, 235–245

18 Regunathan, S. and Reis, D. J. (2000) Characterization of arginine decarboxylase in rat brain and liver: distinction from ornithine decarboxylase. J. Neurochem. **74**, 2201–2208

19 Horyn, O., Luhovyy, B., Lazarow, A., Daikhin, Y., Nissim, I., Yudkoff, M. and Nissim, I. (2005) Biosynthesis of agmatine in isolated mitochondria and perfused rat liver: studies with 15N-labelled arginine. Biochem J. **388**, 419–425

20 Sastre, M., Regunathan, S., Galea, E. and Reis, D. J. (1996) Agmatinase activity in rat brain: a metabolic pathway for the degradation of agmatine. J. Neurochem. **67**, 1761–1765

21 Tesson, F., Limon-Boulez, I., Urban, P., Puype, M., Vanderkerkove, J., Coupry, I., Pompon, D. and Parini, A. (1999) Localization of I2-imidazoline binding sites on monoamine oxidases. J. Biol. Chem. **270**, 9856–9861

22 Schneider, W. C. and Hogeboom, G. H. (1950) Intracellular distribution of enzymes. V. Further studies on the distribution of cytochrome c in rat liver homogenates. J. Biol. Chem. **183**, 123–128

23 Gornall, A. G., Bardawill, C. J. and David, M. M. (1949) Determination of serum proteins by means of the biuret reaction J. Biol. Chem. **177**, 751–766

24 Toninello, A., Salvi, M. and Mondovi, B. (2004) Interaction of biologically active amines with mitochondria and their role in the mitochondrial-mediated pathway of apoptosis. Curr. Med. Chem. **11**, 2349–2374

25 Toninello, A., Di Lisa, F., Siliprandi, D. and Siliprandi, N. (1985) Uptake of spermine by rat liver mitochondria and its influence on the transport of phosphate. Biochim. Biophys. Acta **815**, 399–404

26 Loschen, G., Azzi, A. and Flohè, L. (1973) Mitochondrial H_2O_2 formation: relationship with energy conservation. FEBS Lett. **33**, 84–87

27 Kamo, N., Muratsugu, M., Hongoh, R. and Kobatake, Y. (1979) Membrane potential of mitochondria measured with an electrode sensitive to tetraphenyl phosphonium and relationship between proton electrochemical potential and phosphorylation potential in steady state. J. Membr. Biol. **49**, 105–121

28 Toninello, A., Miotto, G., Siliprandi, D., Siliprandi, N. and Garlid, K. D. (1988) On the mechanism of spermine transport in liver mitochondria. J. Biol. Chem. **263**, 19407–19411

29 Jensen, B. D., Gunter, K. K. and Gunter, T. E. (1986) The efficiencies of the component steps of oxidative phosphorylation. II. Experimental determination of the efficiencies in mitochondria and examination of the equivalence of membrane potential and pH gradient in phosphorylation. Arch. Biochem. Biophys. **248**, 305–323

30 Palmieri, F. and Klingenberg, M. (1979) Direct methods for measuring metabolite transport and distribution in mitochondria. Methods Enzymol. **55**, 279–301

31 Rottenberg, H. (1979) The measurement of membrane potential and δpH in cells, organelles, and vesicles. Methods Enzymol. **55**, 547–569

32 Reich, J. G., Wangermann, G., Falck, M. and Rohde, K. (1972) A general strategy for parameter estimation from isosteric and allosteric kinetic data and binding measurements. Eur. J. Biochem. **26**, 368–379

33 Dalla Via, L., Di Noto, V., Siliprandi, D. and Toninello, A. (1996) Spermine binding to liver mitochondria. Biochim. Biophys. Acta **1284**, 247–252

34 Toninello, A., Dalla Via, L., Siliprandi, D. and Garlid, K. D. (1992) Evidence that spermine, spermidine, and putrescine are transported electrophoretically in mitochondria by a specific polyamine uniporter. J. Biol. Chem. **267**, 18393–18397

35 Garlid, K., Beavis, A. D. and Ratkje, S. K. (1989) On the nature of ion leaks in energy-transducing membranes. Biochim. Biophys. Acta **976**, 109–120

36 Mitchell, P. (1966) Metabolic flow in the mitochondrial multiphase system: an appraisal of the cell-osmotic theory of oxidative phosphorylation. In Regulation of Metabolic Processes in Mitochondria (Tager, J. M., Papa, S., Quagliarello, E. and Slater, E. C., eds.), pp. 65–68, Elsevier Publishing Co., Amsterdam

37 De Marchi, U., Pietrangeli, P., Marcocci, L., Mondovi, B. and Toninello, A. (2003) L-Deprenyl as an inhibitor of menadione-induced permeability transition in liver mitochondria. Biochem. Pharmacol. **66**, 1749–1754

38 Dalla Via, L., Di Noto, V. and Toninello, A. (1999) Binding of spermidine and putrescine to energized liver mitochondria. Arch. Biochem. Biophys. **365**, 482–489

39 Bragadin, M., Pozzan, T. and Azzone, G. F. (1979) Activation energies and enthalpies during Ca^{2+} transport in rat liver mitochondria. FEBS Lett. **104**, 347–351

40 Mende, P., Kolbe, H. V. J., Kadenbach, B., Stipani, I. and Palmieri, F. (1982) Reconstitution of the isolated phosphate-transport system of pig-heart mitochondria. Eur. J. Biochem. **128**, 91–95

41 Palmieri, F., Indiveri, C., Bisaccia, F. and Kramer, R. (1993) Functional properties of purified and reconstituted mitochondrial metabolite carriers. J. Bioenerg. Biomembr. **25**, 525–535

42 Pereira, C. A., Alonso, G. D., Paveto, M. C., Flawia, M. M. and Torres, H. N. (1999) L-arginine uptake and L-phosphoarginine synthesis in *Trypanosoma cruzi*. J. Eukaryot. Microbiol. **46**, 566–570

43 Chan, S. H. and Barbour, R. L. (1983) Adenine nucleotide transport in hepatoma mitochondria. Characterization of factors influencing the kinetics of ADP and ATP uptake. Biochim. Biophys. Acta **723**, 104–113

44 Zhang, W. and Kaback, H. R. (2000) Effect of the lipid phase transition on the lactose permease from *Escherichia coli*. Biochemistry **39**, 14538–14542

45 Klingenberg, M. (2005) Ligand-protein interaction in biomembrane carriers. The induced transition fit of transport catalysis. Biochemistry **44**, 8563–8570

46 Toninello, A., Battaglia, V., Salvi, M., Calheiros, R. and Marques, M. P. (2005) Structural characterization of agmatine at physiological conditions. Struct. Chem. in the press

47 Porter, R. K. (2000) Mammalian mitochondrial inner membrane cationic and neutral amino acid carriers. Biochim. Biophys. Acta **1459**, 356–362

48 Palmieri, F. (2004) The mitochondrial transporter family (SLC25): physiological and pathological implications. Eur. J. Physiol. **447**, 689–709

49 Lortie, M. J., Ishizuke, S., Scwartz, D. and Blantz, R. C. (2000) Bioactive products of arginine in sepsis: tissue and plasma composition after LPS and iNOS blockade. Am. J. Physiol. Cell Physiol. **278**, C1191–C1199

50 Del barre, G., Del barre, B. and Calinon, F. (1995) Determination of agmatine in abdominal aorta of rats and gerbils after ischemic reperfusion insult. Soc. Neurosci. Abs. **21**, 1495

51 Gardini, G., Cabella, C., Cravanzola, C., Vargiu, C., Belliardo, S., Testore, G., Solinas, S. P., Toninello, A., Grillo, M. A. and Colombatto, S. (2001) Agmatine induces apoptosis in rat hepatocyte cultures. J. Hepatol. **35**, 482–489

52 Kim, J. S., He, L. and Lemasters, J. J. (2003) Mitochondrial permeability transition: a common pathway to necrosis and apoptosis. Biochem. Biophys. Res. Commun. **304**, 463–470

53 Coleman, C. S., Hu, G. and Pegg, A. E. (2004) Putrescine biosynthesis in mammalian tissues. Biochem. J. **379**, 849–855

54 Morris, S. M. (2003) Vertebrate agmatinases: what role do they play in agmatine catabolism? Ann. N.Y. Acad. Sci. **1009**, 30–33

55 Nathan, C. (1992) Nitric oxide as a secretory product of mammalian cells. FASEB J. **6**, 3051–3064

56 Marletta, M. A. (1994) Nitric oxide synthase: aspects concerning structure and catalysis. Cell **78**, 927–930

57 Lacza, Z., Puskar, M., Figueroa, J. P., Zhang, J., Rajapakse, N. and Busija, D. W. (2001) Mitochondrial nitric oxide synthase is constitutively active and is functionally upregulated in hypoxia. Free Radic. Biol. Med. **31**, 1609–1615

58 Carreras, M. C., Franco, M. C., Peralta, J. G. and Poderoso, J. J. (2004) Nitric oxide, complex I, and the modulation of mitochondrial reactive species in biology and disease. Mol. Asp. Med. **25**, 125–139

Received 3 January 2006/22 February 2006; accepted 2 March 2006
Published as BJ Immediate Publication 2 March 2006, doi:10.1042/BJ20060003